J. Phys. D: Appl. Phys. 28 (1995) 1729–1736. Printed in the UK

Characterizing multi-mode resonant-mass gravitational wave detectors

Michael E Tobar

Department of Physics, University of Western Australia, Nedlands 6009, Western Australia

Received 29 November 1994

Abstract. This paper presents general techniques to assist in characterizing multi-mode resonant-mass gravitational wave detectors. From measurements of normal mode frequencies, lumped element frequencies and masses can be determined. From measurements of normal mode Q values, the lumped element Q values can also be determined. Once the system has been characterized it is then possible to calculate the normal mode effective masses and electromechanical couplings which are essential for an accurate calibration and sensitivity determination. The presented method is shown to be consistent with experiments on the UWA gravitational wave detector (a two-mode system). The method is also implemented with respect to a three-mode system, and the characteristics of an upgraded UWA detector with a two-mode sapphire transducer are investigated.

1. Introduction

The possibility of detecting gravitational radiation was first proposed by Weber in 1960 [1] who built two single-mode resonant-mass gravity wave (GW) detectors made from large aluminium cylinders which operated at room temperature. To convert vibrations of the cylindrical antenna to an electrical signal he used piezoelectric crystals as an electromechanical device.

The next generation of detectors were built for cryogenic operation and had a second smaller tuned resonant mass attached to the end (two-mode antenna). The secondary mass acts as a resonant transformer, amplifying the primary mass vibrations and thereby improving the impedance match to the electromechanical transducer [2]. The cryogenic operation allowed the development of superconducting electromechanical devices; such as RF SQUIDs coupled to mechanically modulated inductive and capacitive devices [3–5], and capacitive modulated microwave cavities [6].

The first cryogenic two-mode antenna to operate for an extended period was at Stanford in 1980, and again in 1984–5 [7]. In 1986 two-mode cryogenic detectors were operating in Rome (Explorer), Louisiana (Allegro) and Stanford, and the first three-way coincidence was performed [8]. However the best limit to the flux of GW radiation originates from an 18-month coincidence between Explorer and Allegro from June 1991 [9]. Both these detectors were operating with a 1 ms burst sensitivity of $h_{1\mathrm{ms}} < 10^{-18}$. No significant coincidence (less than one event every ten days) above $h_{1\mathrm{ms}} = 3 \times 10^{-18}$ between the two detectors was observed. Currently there are three two-mode antennas operating with burst sensitivities of about $h_{1\mathrm{ms}} = 7 \times 10^{-19}$, with approximately a 1 Hz bandwidth. They are Explorer, Allegro and the UWA gravitational wave detector.

Two-mode antennas can only achieve bandwidths of around 10 to 20 Hz. It has been shown that the bandwidth and sensitivity of resonant-mass detectors can be increased [10–14] by adding additional modes. The increased bandwidth is necessary if resonant-mass detectors are going to be used to search for any other sources besides bursts. Three to five mode devices have been considered and are now currently under development at Maryland, Louisiana, Rochester and Italy [10–15]. Researchers at Louisiana soon plan to change their current two-mode antenna (Allegro) to a three-mode device by replacing their single resonant transducer with a two-mode resonant transducer [14]. Calculations suggest they can achieve a 70 Hz bandwidth with a burst sensitivity of $h_{1\mathrm{ms}} < 10^{-19}$.

Researchers in the resonant-mass GW community are now focusing on building transducers that increase the bandwidth of resonant-mass detectors. This paper shows how the general multi-mode system can be characterized and calibrated from measurements. The model is shown to be consistent with results from the two-mode detector at UWA. It is also used to investigate the characteristics of the UWA antenna extended to a three-mode system.

2. Equation of motion

The lumped model of a multi-mode resonant-mass GW detector with n lumped elements is shown in figure 1. For the ith lumped element we define: m_i, the effective

0022-3727/95/081729+08$19.50

mass; k_i, the spring constant; h_i, the dissipation constant; $\omega_i = (k_i/m_i)^{1/2}$, the resonant frequency of the ith element with respect to an infinite wall; $\tau_i = 2m_i/h_i$ the amplitude decay time constant; $Q_i = \tau_i\omega_i/2$ the acoustic Q. Defining the displacement of the ith lumped element as x_i the equation of motion for this system may be written as the following $2n \times 2n$ first-order differential matrix equation:

$$\dot{x}_{2n} = A_{2n}x_{2n} + B_{2n\times n}f_n \tag{1}$$

where

$$x_{2n} = \begin{bmatrix} x_1 \\ \dot{x}_n \\ x_{n+1} \\ \dot{x}_{2n} \end{bmatrix} \qquad A_{2n} = \begin{bmatrix} \mathbf{0}_n I_n \\ \Omega_n T_n \end{bmatrix}$$

$$B_{2n\times n} = \begin{bmatrix} \mathbf{0}_n \\ M_n \end{bmatrix} \qquad f_n = \begin{bmatrix} F_1 \\ \cdot \\ F_n \end{bmatrix}.$$

Here $x_{n+i} = \dot{x}_i$ ($i = 1$ to n) and F_i is the force input at each element. Also $\mathbf{0}_n$ and I_n are the zero and unity $n \times n$ matrices respectively; Ω_n is an $n \times n$ tri-diagonal matrix which depends on lumped element resonant frequencies and effective masses; T_n is an $n \times n$ tridiagonal matrix depends on element decay times and effective masses; M_n is an $n \times n$ diagonal matrix which only depends on lumped element effective masses. These matrices are given by

$$\Omega_n = \begin{bmatrix} -\omega_1^2 - \frac{m_2}{m_1}\omega_2^2 & \frac{m_2}{m_1}\omega_2^2 & 0\dots \\ \cdot & \cdot & \cdot \\ 0\dots\omega_{n-1}^2 & -\omega_{n-1}^2 - \frac{m_n}{m_{n-1}}\omega_n^2 & \frac{m_n}{m_{n-1}}\omega_{n-1}^2 \\ 0\dots & \dots\omega_n^2 & -\omega_n^2 \end{bmatrix}$$

$$T_n = \begin{bmatrix} -\frac{2}{\tau_1} - \frac{2m_2}{m_1\tau_2} & \frac{2m_2}{m_1\tau_2} & 0\dots \\ \cdot & \cdot & \cdot \\ 0\dots\frac{2}{\tau_{n-1}} & -\frac{2}{\tau_{n-1}} - \frac{2m_n}{m_{n-1}\tau_n} & \frac{2m_n}{m_{n-1}\tau_{n-1}} \\ 0\dots & \dots\frac{2}{\tau_n} & -\frac{2}{\tau_n} \end{bmatrix}$$

$$M_n = \begin{bmatrix} \frac{1}{m_1} & 0\dots & & \\ 0 & \frac{1}{m_2} & 0 & \dots \\ & & \cdot & \\ 0 & \dots & \dots & \frac{1}{m_{n-1}} \quad 0 \\ 0 & \dots & \dots & \dots \quad \frac{1}{m_n} \end{bmatrix}.$$

Equation (1) is the equation of motion for a lumped spring-mass system consisting of n elements. When constructing such a system these individual elements may be measured or estimated separately. However, once the elements have been combined in a working system, the uncertainties in these values may be large. The assembled elements form a coupled oscillator system, and the measured normal modes have contributions from each lumped element. The normal mode characteristics may be measured directly with an accuracy only limited by the measurement precision. In sections 3 to 5 a method is developed which enables precise characterization of the individual lumped elements from measurements of the normal modes for a general n-mode system.

3. Normal mode electro-mechanical couplings

A multi-mode GW detector will be designed with a massive primary mass possessing a significant cross section to gravitational radiation, and an $n-1$ mode resonant transducer to amplify the primary mass vibrations (figure 1). If the $n-1$ mode resonant transducer is to amplify the vibrations of the primary mass then the following is usually true

$$m_1 > m_2 \dots > m_{n-1} > m_n. \tag{2}$$

If the individual uncoupled resonant frequencies of the lumped elements can be perturbed (i.e. by perturbing the spring constant or mass of an element), then this gives the experimenter further information from which to characterize the system. Given that equation (2) is true, in a tuned system element m_n will always have the smallest inertia and spring constant. Subsequently it is assumed that m_n may be perturbed without significantly influencing any of the proceeding mass elements. It is emphasized here that the proceeding calculations do not assume that equation (2) is true, the only assumption necessary is that the nth element may be perturbed independently of others.

The fractional perturbation in the measured normal mode frequencies due to small perturbations in the nth lumped element frequency is given by

$$\frac{\Delta\omega_{nmi}}{\omega_{nmi}} = \frac{\partial\omega_{nmi}}{\partial\omega_n}\frac{\Delta\omega_n}{\omega_{nmi}}. \tag{3}$$

Usually the nth lumped element will be coupled to an electromechanical transducer. One way to perturb a resonant mass frequency is by altering the spring constant of the nth lumped element with a reactively coupled electromechanical transducer. The amount of perturbation depends on the imaginary part of the transducer's input impedance [16], and for small perturbations is given by

$$\Delta\omega = \Delta\,\mathrm{Im}(Z_{in})/(2m_n) \tag{4}$$

here Z_{in} is the input impedance of the nth lumped element to the transducer. Usually the nth element is the only significant component of the input impedance due to the transducer being coupled directly to it, and also because of condition (2).

The input impedance per kilogramme ($Z_n = Z_{in}/m_n[\mathrm{s}^{-1}]$) can be shown to be proportional to the product of the electromechanical coupling and frequency of the nth lumped element (the electromechanical coupling of the other $n-1$ elements are negligible) [17]. Thus small perturbations in the imaginary part of the input impedance can be expressed as

$$\Delta\,\mathrm{Im}(Z_n) = \beta_n\omega_n\alpha_n \tag{5}$$

where β_n is the electromechanical coupling of the nth element to the electrical transducer, and α_n is the proportionality constant which will depend on the type of electrical transducer and its regime of operation. The input impedance of the coupled mode system, which is given mainly by the nth lumped element, must be split amongst the normal modes (and is thus equal to the sum of the

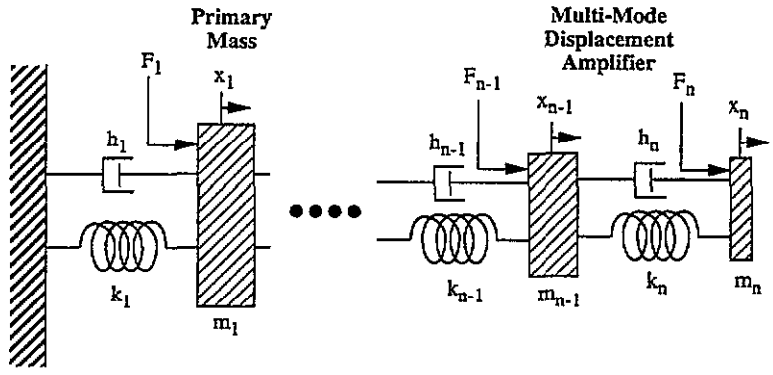

Figure 1. Lumped element model of a multi-mode gravitational wave antenna with n lumped elements. The detector consists of a primary resonant mass which is sensitive to gravitational radiation, and an $n-1$ mode resonant displacement amplifier.

normal mode input impedances). The perturbation of the input impedance may therefore be expressed in terms of perturbations of the normal mode input impedances (Z_{nmi}) as

$$\Delta \operatorname{Im}(Z_n) \approx \sum_{i=1}^{n} \Delta \operatorname{Im}(Z_{nmi}) = \alpha_n \sum_{i=1}^{n} \beta_{nmi}\omega_{nmi} \qquad (6)$$

where β_{nmi} is the ith normal mode electromechanical coupling to the electrical transducer. Because the normal modes all 'see' the same transducer they must have the same proportionality constant α_n relating the electromechanical coupling to the input impedance.

By substituting equation (5) into equation (4) the frequency perturbation of the nth lumped element can be shown to be proportional to the product of its electromechanical coupling and resonant frequency

$$\Delta\omega_n = \beta_n\omega_n\alpha_n/2. \qquad (7)$$

Then by substituting the change in the ith normal mode input impedance into equation (4) the perturbation of the normal mode frequency can be shown to be proportional to the product of the normal mode electromechanical coupling and resonant frequency

$$\Delta\omega_{nmi} = \beta_{nmi}\omega_{nmi}\alpha_n/2. \qquad (8)$$

Thus the fractional normal mode electromechanical couplings may be calculated from equation (9) by substituting equations (7) and (8) into equation (3)

$$\frac{\beta_{nmi}}{\beta_n} = \frac{\partial\omega_{nmi}}{\partial\omega_n}\frac{\omega_n}{\omega_{nmi}}. \qquad (9)$$

Equation (9) is a general equation for calculating the electromechanical couplings of the detector's normal modes. Also, given that the following must be true

$$\beta_n \approx \sum_{i=1}^{n} \beta_{nmi} \qquad (10)$$

then the following relation is implied from equations (9) and (10)

$$\sum_{i=1}^{n} \frac{\partial\omega_{nmi}}{\partial\omega_n}\frac{\omega_n}{\omega_{nmi}} = 1. \qquad (11)$$

This condition is the same as the geometric mean of the uncoupled frequencies being equal to the geometric mean of the normal mode frequencies, which is always true and is derived later in equation (15a), i.e. if we take the natural log of both sides and partially differentiate (15a) with respect to ω_n, then equation (11) can be shown to be true.

The normal mode frequencies of such a system can be accurately measured experimentally. However, the individual lumped element parameters are not necessarily well known. Likewise, the magnitude of a small perturbation of the nth lumped element may be difficult to determine accurately. Since the perturbations in the normal mode frequencies can be accurately measured, the ratio of normal mode couplings can in principle be calculated very precisely, as they only depend on the normal mode measurements. From equations (9) and (3) the electromechanical coupling ratios may be written as

$$\kappa_{ij} = \beta_{nmi}/\beta_{nmj} = \frac{\Delta\omega_{nmi}}{\Delta\omega_{nmj}}\frac{\omega_{nmj}}{\omega_{nmi}}. \qquad (12)$$

In the following sections it will be shown that from measurements of the normal mode frequencies, Q factors, and normal mode coupling ratios, sufficient information is obtained to characterize an n-mode mass–spring system such as a gravitational wave detector.

4. Resonant-mass frequencies, Q values and effective mass ratios

The characteristic equation of the equation of motion is of the form

$$s^{2n} + a_1 s^{2n-1} + \cdots + a_{2n}. \qquad (13)$$

The coefficients a_i are determined from $\det[sI_{2n} - A_{2n}] = 0$, where A_{2n} is the $2n \times 2n$ matrix in the equation of motion (1) and I_{2n} is a $2n \times 2n$ unity matrix. To calculate the normal mode frequencies and decay times from the uncoupled parameters we equate the coefficients of equation (13) to the coefficients of the normal mode characteristic equation given by

$$\prod_{i=1}^{n} s^2 + \frac{2}{\tau_{nmi}}s + \omega_{nmi}^2. \qquad (14)$$

Ignoring terms of order Q^{-2}, equating even coefficients creates a polynomial of order n that can be used to solve for the frequencies, and equating odd terms creates a matrix equation that can be used to solve for the amplitude decay times or Q values.

Equating coefficients of the even powers of equations (14) and (13) leads to the following set of n equations (ignoring terms of order Q^{-2}):

$$s^0 \qquad \prod_{i=1}^{n} \omega_i^2 = \prod_{i=1}^{n} \omega_{nmi}^2 \tag{15a}$$

$$s^2 \qquad \sum_{i=1}^{n} c_i/\omega_i^2 = \sum_{i=1}^{n} 1/\omega_{nmi}^2$$
$$(c_n = 1 \text{ and } c_{k-1} = c_k \mu_{kk-1} + 1) \tag{15b}$$

$$\vdots$$

$$s^{2n} \qquad \sum_{i=1}^{n} \omega_i^2 (1 + \mu_{ii-1}) = \sum_{i=1}^{n} \omega_{nmi}^2. \tag{15c}$$

Here we define the effective mass ratio between adjacent elements as $\mu_{ii-1} = m_i/m_{i-1}$, where $m_0 = \infty$ as m_1 is attached to an infinite wall. Implicitly differentiating equations (15a) and (15b) with respect to ω_n, the frequency of the nth lumped element can be calculated to be

$$\omega_n^2 = \frac{\sum_{i=1}^{n} \kappa_{ij}}{\sum_{i=1}^{n} \kappa_{ij}/\omega_{nmi}^2}. \tag{16}$$

Now by implicitly differentiating equation (15c) and substituting in equation (16), the effective mass ratio between the nth and $n-1$th element can be calculated to be

$$\mu_{nn-1} = \frac{\left(\sum_{i=1}^{n} \omega_{nmi}^2 \kappa_{ij}\right)\left(\sum_{i=1}^{n} \kappa_{ij}/\omega_{nmi}^2\right)}{\left(\sum_{i=1}^{n} \kappa_{ij}\right)^2} - 1. \tag{17}$$

By substituting equations (17) and (16) back into equations (15) the entire system can be solved, i.e. the rest of the uncoupled element frequencies and effective mass ratios can be calculated. The author has done this for up to $n = 4$, and in sections 6 and 7 cases when $n = 2$ and $n = 3$ are presented.

Once the frequency and mass ratios have been solved, the odd coefficients in equations (13) and (14) can be equated to solve for the lumped element decay times. Ignoring terms of order τ^{-2}, a matrix equation of the following form can be derived

$$P_n \underline{\tau}_{inv} = Z_n \underline{\tau}_{invnm}. \tag{18}$$

Here P_n is an $n \times n$ matrix that depends on the lumped element resonant frequencies and effective mass ratios, $\underline{\tau}_{inv}$ is an n vector of lumped element inverse amplitude decay times, Z_n is an $n \times n$ matrix that depends on the normal mode resonant frequencies, and $\underline{\tau}_{invnm}$ is an n vector of normal mode inverse amplitude decay times. The matrices P_n and Z_n can both be determined from measured normal mode parameters as described above. Thus from measurements of the normal mode amplitude decay times, the lumped element decay times can be determined by inverting the matrix P_n in equation (18). In sections 6 and 7 this is done for two- and three-mode systems respectively.

5. Normal mode effective masses

In this section general equations are derived to calculate the normal mode masses of a multi-mode gravitational wave detector assuming that the detector is in thermal equilibrium with its surroundings, and the electromechanical sensor attached to the detector will mainly detect the displacement of the nth lumped element. Thus the normal mode values quoted here are the values with respect to the nth lumped element.

When the resonant-mass detector is in thermal equilibrium at temperature T, there will be kT of energy in each normal mode. Thus defining the normal mode masses (m_{nmi}) and displacements (x_{nmi}) with respect to the nth lumped element, by Nyquist's theorem:

$$kT = m_{nmi} \omega_{nmi}^2 \langle x_{nmi}^2 \rangle. \tag{19}$$

Considering the nth lumped element separately in equilibrium with its surroundings, then also

$$kT = m_n \omega_n^2 \langle x_n^2 \rangle. \tag{20}$$

Thus the ratio of the mean square displacements is given by

$$\frac{\langle x_{nmi}^2 \rangle}{\langle x_n^2 \rangle} = \frac{m_n \omega_n^2}{m_{nmi} \omega_{nmi}^2}. \tag{21}$$

Assuming that the electromechanical coupling sensed by the transducer is proportional to the mean square displacement, then equating equations (21) and (9) gives

$$\frac{m_{nmi}}{m_n} = \left(\frac{\partial \omega_{nmi}}{\partial \omega_n} \frac{\omega_{nmi}}{\omega_n}\right)^{-1}. \tag{22}$$

Rearranging equation (22) and summing over all normal modes one can show that

$$\frac{1}{m_n \omega_n^2} = \sum_{i=1}^{n} \frac{1}{m_{nmi} \omega_{nmi}^2} \tag{23}$$

which is equivalent to

$$\langle x_n^2 \rangle = \sum_{i=1}^{n} \langle x_{nmi}^2 \rangle \tag{24}$$

as expected.

Thus from the knowledge of the effective mass of the last lumped element, the normal mode masses may be calculated from equation (22).

6. Consistency of the model with the UWA detector

By perturbing the normal mode frequencies of the UWA gravitational wave antenna, calculations of frequencies and Q values for the $n = 2$ case have been shown to be consistent with experiments [17, 18]. The UWA antenna has been described in detail elsewhere [19, 20]. Basically it consists of a niobium bending flap of 0.45 kg effective mass tuned near to the fundamental frequency of a 1.5 tonne niobium resonant bar, configured with a 9.5 GHz re-entrant cavity parametric transducer.

Table 1. Measured parameters of the UWA GW detector, for two experimental series.

Measured parameters	1991	1993/94
$\omega_+/2\pi$ (Hz)	711.334	713.106
$\omega_-/2\pi$ (Hz)	688.859	694.673
$Q_+(\times 10^7)$	1.6 ± 0.05	3.0 ± 0.05
$Q_-(\times 10^7)$	0.37 ± 0.01	1.4 ± 0.05
κ_{+-}	0.213	0.413
Q_1	$(2.3 \pm 0.3) \times 10^8$	
$\omega_1/2\pi$ (Hz)	709.7	
m_1 (kg)	755	

Table 2. Calculated parameters of the UWA GW detector from the two-mode model for two experimental runs. The discrepancy between the calculated and measured bar frequency is due to mass loading of the bending flap base.

Calculated parameters	1991	1993/94
$\omega_1/2\pi$ (Hz)	707.5	707.7
$\omega_2/2\pi$ (Hz)	692.6	699.9
$Q_1(\times 10^7)$	20 ± 1	20 ± 0.5
$Q_2(\times 10^7)$	0.31 ± 0.01	1.0 ± 0.05
m_2 (kg)	0.45	0.43

For the two-mode model the following equations follow from equations (16) and (17):

$$\omega_2^2 = \frac{1+\kappa_{+-}}{1/\omega_-^2 + \kappa_{+-}/\omega_+^2} \tag{25}$$

$$1+\mu_{21} = \frac{(1/\omega_-^2 + \kappa_{+-}/\omega_+^2)(\omega_-^2 + \kappa_{+-}\omega_+^2)}{(1+\kappa_{+-})^2}. \tag{26}$$

Then from equations (15*a*) and (25) the primary mass frequency can be determined to be

$$\omega_1^2 = \frac{\omega_+^2/\kappa_{+-} + \omega_-^2}{1 + 1/\kappa_{+-}}. \tag{27}$$

Equations (25) to (26) give simple equations that allow characterization of the lumped element frequencies and mass ratio for a two-mode system. Once these have been calculated, equation (18) can be used to calculate the lumped element amplitude decay times from measurements of the normal mode decay times. For a two-mode system, equation (18) becomes

$$\begin{bmatrix} 1 & 1+\mu_{21} \\ 1/\omega_1^2 & 1/\omega_2^2 \end{bmatrix} \begin{bmatrix} 1/\tau_1 \\ 1/\tau_2 \end{bmatrix} = \begin{bmatrix} 1 & 1 \\ 1/\omega_+^2 & 1/\omega_-^2 \end{bmatrix} \begin{bmatrix} 1/\tau_+ \\ 1/\tau_- \end{bmatrix}. \tag{28}$$

In past experiments variations of equations (25)–(28) have been used to characterize the UWA gravitational wave detector by perturbing the normal modes with a parametric transducer [17, 18]. Table 1 summarizes the measured normal mode parameters for a past experimental run in 1991, and the current experiment which began in 1993. The measured niobium bar parameters before the transducer was attached are also included. Table 2 presents the calculated lumped element parameters from equations (25)–(28) from the measured parameters.

The current values for the 1993/94 experimental run are consistent with the 1991 experiment. Between these experiments the bending flap was etched to tune it closer to the bar frequency [21]. For perfect tuning the ratio of the electromechanical couplings of the two normal modes κ_{+-} should be approximately one.

Equation (9) allows the calculation of the normal mode electromechanical couplings. Since the normal mode frequencies of a two-mode system may be calculated analytically in terms of the lumped elements, the dependency of the normalized mode couplings as a function of secondary mass frequency may be plotted directly as shown in figure 2.

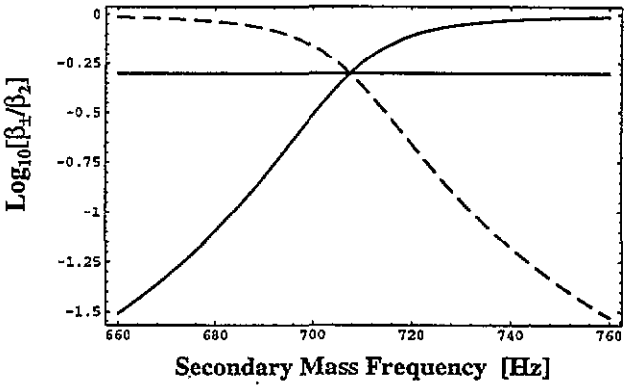

Figure 2. Normalized mode couplings as a function of secondary mass frequency. The full curve represents the + mode and the broken curve represents the − mode. The horizontal line is when $\kappa_{+-} = 1$ (nearly perfectly tuned), at this point $\beta_+ = \beta_- = \beta_2/2$.

To calibrate the UWA antenna we make use of the self-calibrating properties of the re-entrant cavity microwave transducer. The transducer is configured to maximize the voltage–frequency response $\mathrm{d}v/\mathrm{d}f$ (V Hz^{-1}). This quantity is measured by frequency sweeping the pump across the transducer resonance and measuring the voltage frequency slope at the required pump operating point. From this measurement the displacement sensed by the transducer can be calculated from

$$\delta x_\pm = \mathrm{d}f/\mathrm{d}v(\mathrm{d}f/\mathrm{d}x)^{-1}\delta v_\pm. \tag{29}$$

Here $\delta v_\pm$ is the measured voltage response of the normal modes, and $\mathrm{d}f/\mathrm{d}x$ is the displacement sensitivity of the re-entrant cavity transducer ($\mathrm{d}f/\mathrm{d}x \sim 300$ MHz μm^{-1}). To first order, $\mathrm{d}f/\mathrm{d}x$ is independent of temperature and can be measured at room temperature. By observing the re-entrant cavity frequency shift from room temperature to 5 K, any second-order change in $\mathrm{d}f/\mathrm{d}x$ can then be calculated.

The energy in the normal modes of the oscillator is given by (where k is Boltzmann's constant)

$$E_\pm = kT_\pm/2 = (m_\pm\omega_\pm^2\delta x_\pm^2)/2 \tag{30a}$$

and in terms of the normal mode temperatures by

$$T_\pm = (m_\pm\omega_\pm^2\delta x_\pm^2)/k \tag{30b}$$

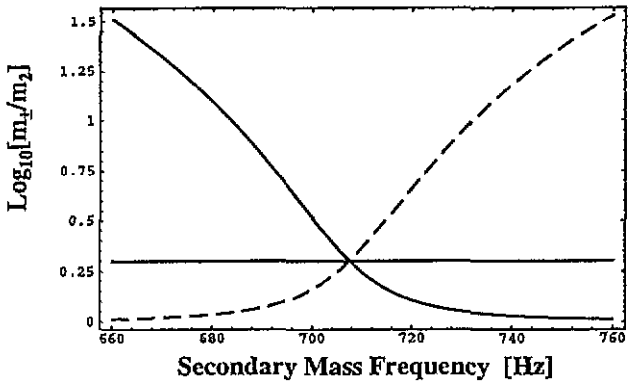

Figure 3. Normalized normal mode masses as a function of secondary mass frequency. The full curve represents the + mode and the broken curve represents the − mode. The horizontal line is when $\kappa_{12} = 1$ (nearly perfectly tuned) and at this point $m_+ = m_- \approx 2m_2$.

where $m_\pm$ are the normal mode masses. Equation (22) allows for the calculation of the normal mode masses, which are shown as a function of secondary mass frequency in figure 3. If the bar and the bending flap were perfectly tuned, both modes would amplify displacements of the bar by $\sqrt{\mu_{12}}$, with their normal mode masses given by $m_\pm = 2m_2$. If the flap is detuned from the bar; when $\omega_1 \gg \omega_2$ the bar becomes an infinite wall with respect to the flap, and $m_- \to m_2$, $m_+ \to \infty$; when $\omega_2 \gg \omega_1$ the flap becomes stiff with respect to the bar and does not act as a displacement amplifier, and $m_+ \to m_2$, $m_- \to \infty$.

Calculation of the normal mode masses is important because they give a simple way of calibrating the detector if the transducer displacement sensitivity is known, or verifying another calibration method. Equation (22) may be compared with a previous result for a two-mode system [22], given by

$$m_\pm = \frac{m_1 + m_2\lambda_\pm^2}{(\lambda_\pm^2 - 1)^2} \qquad \lambda_\pm = \frac{\omega_2^2}{\omega_2^2 - \omega_\pm^2}. \tag{31}$$

When this calculation is plotted with equation (22) shown in figure 3, no visible difference between the two calculations can be seen, verifying equation (22) for the $n = 2$ case. However, equation (22) is a general calculation that may be used for a multi-mode system.

7. A three-mode detector as an example

Research groups constructing large scale resonant-mass detectors are now investigating and developing detectors with more than two resonant modes [14, 23]. In this section we give an example of how the method presented in this paper may be used to characterize and calibrate a three-mode detector. A three-mode tuned resonant-mass system will consist of lower, central and upper normal modes, which we denote in this section by subscripts −, 0, and + respectively.

For the three-mode model the following equations follow from equations (16) and (17):

$$\omega_3^2 = \frac{1 + \kappa_{+0} + \kappa_{-0}}{1/\omega_0^2 + \kappa_{+0}/\omega_+^2 + \kappa_{-0}/\omega_-^2} \tag{32}$$

$$1 + \mu_{32} = \frac{(1/\omega_0^2 + \kappa_{+0}/\omega_+^2 + \kappa_{-0}/\omega_-^2)(\omega_0^2 + \kappa_{+0}\omega_+^2 + \kappa_{-0}\omega_-^2)}{(1 + \kappa_{+0} + \kappa_{-0})^2}. \tag{33}$$

From substitutions into equations (15), the rest of the lumped element frequencies and effective mass ratios may be solved:

$$\omega_1^2 = \frac{\omega_+^2/\kappa_{+0}(\omega_0^2-\omega_-^2)^2+\omega_-^2/\kappa_{-0}(\omega_+^2-\omega_0^2)^2+\omega_0^2(\omega_+^2-\omega_-^2)^2}{(\omega_0^2 - \omega_-^2)^2/\kappa_{+0} + (\omega_+^2 - \omega_0^2)^2/\kappa_{-0} + (\omega_+^2 - \omega_-^2)^2} \tag{34}$$

$$\omega_2^2 = \frac{\omega_+^2\omega_0^2\omega_-^2}{\omega_1^2\omega_3^2} \tag{35}$$

$$1 + \mu_{21} = [\omega_+^2 + \omega_0^2 + \omega_-^2 - \omega_1^2 - (1 + \mu_{32})\omega_3^2]\omega_2^{-2}. \tag{36}$$

Equations (32) to (36) give simple equations that allow characterization of the lumped element frequencies and mass ratio for a three-mode system. Once these have been calculated, equation (18) can be used to calculate the lumped element amplitude decay times from measurements of the normal mode decay times. For a three-mode system, equation (18) becomes

$$\begin{bmatrix} 1 & 1 + \mu_{21} & \\ \omega_2^2 + \omega_3^2(1 + \mu_{32}) & \omega_1^2 + \omega_3^2[1 + \mu_{21}(1 + \mu_{32})] & \\ 1/\omega_1^2 & 1/\omega_2^2 & \\ & 1 + \mu_{32} & \\ & \omega_1^2(1 + \mu_{32}) + \omega_2^2[1 + \mu_{21}(1 + \mu_{32})] & \\ & 1/\omega_3^2 & \end{bmatrix} \begin{bmatrix} 1/\tau_1 \\ 1/\tau_2 \\ 1/\tau_3 \end{bmatrix} = \begin{bmatrix} 1 & 1 & 1 \\ \omega_0^2 + \omega_-^2 & \omega_+^2 + \omega_-^2 & \omega_+^2 + \omega_0^2 \\ 1/\omega_+^2 & 1/\omega_0^2 & 1/\omega_-^2 \end{bmatrix} \begin{bmatrix} 1/\tau_+ \\ 1/\tau_0 \\ 1/\tau_- \end{bmatrix}. \tag{37}$$

Once the system has been characterized, equations (9) and (22) can be used to calculate the normal mode couplings and masses for $n = 3$. The normal mode masses can then be used to calibrate the detector in a similar way to the UWA two-mode example given in section 6.

7.1. Characteristics of the UWA niobium antenna with a two-mode sapphire transducer

The possibility of changing the current UWA detector to a three-mode detector has been discussed recently, with a projected 1 ms burst strain sensitivity of about 4×10^{-20} [23]. This suggestion is based on attaching a two-mode sapphire transducer to the 1.5 tonne Nb antenna at UWA. In this section equations (9), (22) and (32)–(37) are used in reverse to investigate the expected normal mode behaviour from the coarsely designed lumped element values.

The lumped element values of the niobium resonant bar are $\omega_1/2\pi = 708.5$ Hz, $m_1 = 755$ kg, $Q_1 = 2 \times 10^8$. Approximate design values for the proposed two-mode resonant transducer can be targeted. Initially it is assumed that the tertiary and secondary sapphire masses can be tuned such that $\omega_3/2\pi = \omega_2/2\pi = \omega_1/2\pi = 708.5$ Hz. The tertiary and secondary mass are assumed to have effective masses of $m_3 = 0.05$ kg and $m_2 = 6$ kg respectively. The acoustic Q value of sapphire has been measured previously

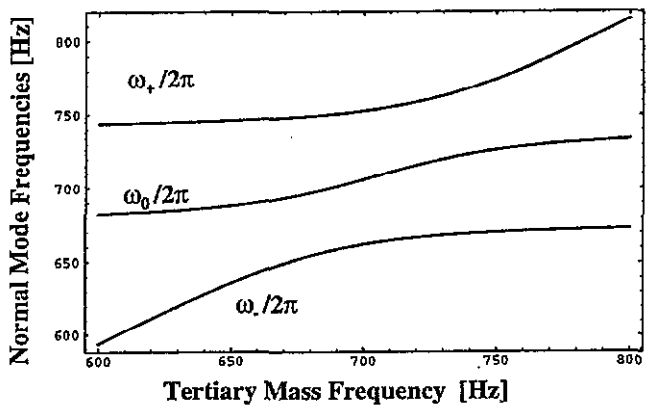

Figure 4. Normal mode frequencies against tertiary mass frequency for the UWA antenna with the proposed two-mode sapphire transducer.

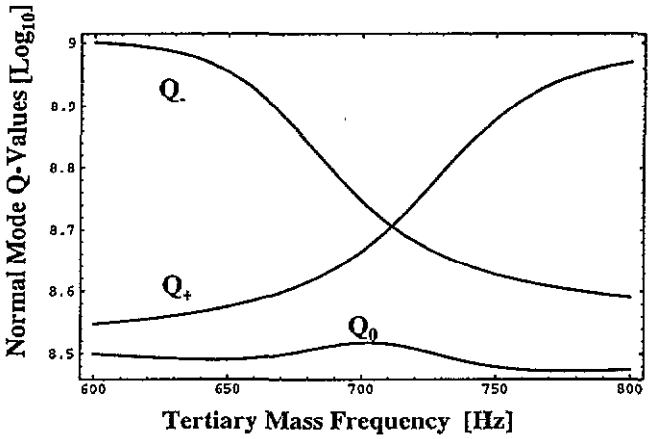

Figure 5. Normal mode Q values against tertiary mass frequency for the UWA antenna with the proposed two-mode sapphire transducer.

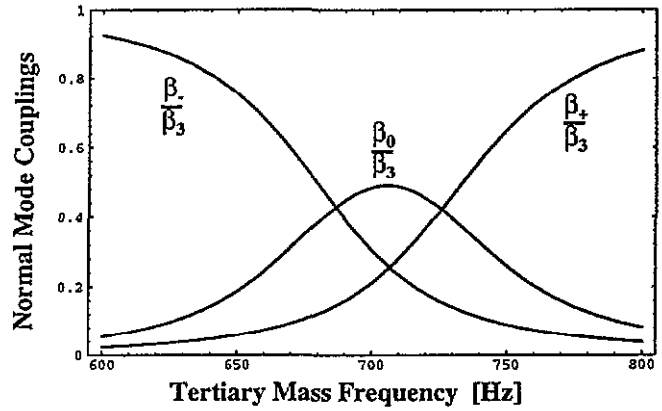

Figure 6. Normalized electromechanical couplings of the normal modes against tertiary mass frequency for the UWA antenna with the proposed two-mode sapphire transducer.

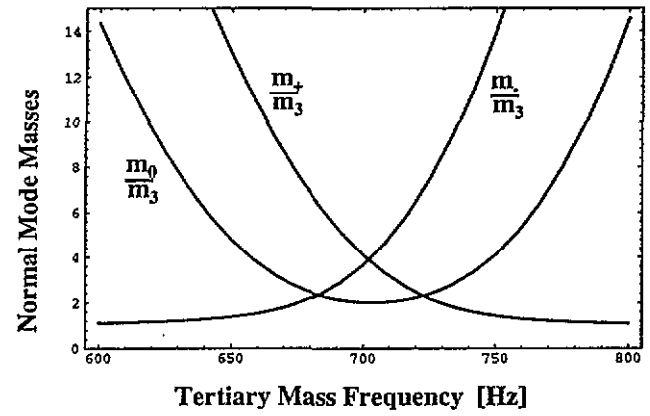

Figure 7. Normalized normal mode masses versus tertiary mass frequency for the UWA antenna with the proposed two-mode sapphire transducer.

at 4 K [24] and exceeds 10^9; thus it will be assumed here that $Q_3 = Q_2 = 10^9$.

Solving the cubic equation gives the normal mode frequencies to be $\omega_+/2\pi = 754.404$ Hz, $\omega_0/2\pi = 709.941$ Hz and $\omega_-/2\pi = 664.038$ Hz. Then, from equation (37) the normal mode Q values are calculated to be $Q_+ = 4.9 \times 10^9$, $Q_0 = 3.3 \times 10^9$, $Q_- = 5.2 \times 10^8$. Next, the normal mode effective masses may be calculated by numerically or analytically calculating $\partial\omega_{-0+}/\partial\omega_3$ and substituting into equation (22). The normal mode masses of this system are calculated to be $m_+/m_3 = 3.74$, $m_0/m_3 = 2.04$ and $m_-/m_3 = 4.68$, and the normal mode electromechanical couplings are calculated to be $\beta_+/\beta_3 = 0.27$, $\beta_0/\beta_3 = 0.49$ and $\beta_-/\beta_3 = 0.24$.

Figures 4 to 7 show how all these normal mode parameters change as the frequency of the third mass element is varied with all other elements held constant.

8. Conclusion

A theoretical method has been presented that allows the characterization and calibration of a multi-mode gravitational wave detector. From measurements of the normal mode resonant frequencies and Q values, the lumped element frequencies, Q values, mass ratios, normal mode masses and electromechanical couplings may be calculated. This model has proved to be consistent with the two-mode UWA gravity wave detector. An example of how the method could be used to characterize a three-mode detector is given. The characteristics of a proposed three-mode extension of the UWA GW detector have also been analysed.

Acknowledgments

The author thanks the rest of the UWA gravity wave group—David Blair, Ik Siong Heng, Eugene Ivanov, Frank van Kann, Nick Linthorne and Peter Turner—for their help and incentive to produce this work. This work was supported by the Australian Research Council.

References

[1] Weber J 1960 Detection and generation of gravitational waves *Phys. Rev.* **117** 306

[2] Paik H J 1974 Analysis and development of a very sensitive low temperature gravitational wave detector *PhD Thesis* Stanford University

[3] Michelson P F and Taber R C 1981 Sensitivity analysis of a resonant mass gravitational wave antenna with resonant transducer *J. Appl. Phys.* **52** 4313–9

[4] Rapagnani P 1982 Development and test at $T = 4.2$ K of a capacitive resonant transducer for cryogenic gravitational-wave antennas *Nuovo Cimento* C **5** 385–408
[5] Astone P *et al* 1993 Long term operation of the Rome Explorer cryogenic gravitational wave detector *Phys. Rev.* D **47** 362–75
[6] Veitch P J, Blair D G, Linthorne N P, Mann L D and Ramm D K 1987 Development of a 1.5 tonne niobium gravitational radiational antenna *Rev. Sci. Instrum.* **58** 1910
[7] Michelson P F and Taber R C 1981 'Can a resonant-mass gravitational-wave detector have wide band sensitivity?' *J. Appl. Phys.* **52** 4313–9
[8] Amaldi E *et al* 1989 First gravity wave coincidence experiment between resonant cryogenic detectors: Louisiana–Rome–Stanford *Astron Astrophys.* **216** 325
[9] Astone P *et al* 1992 Results of a preliminary data analysis in coincidence between the LSU and Rome gravitational wave antennas *Proc. 10th Italian Conf. on General Relativity and Gravitational Physics*
[10] Richard J-P 1984 *Phys. Rev. Lett.* **52** 165
[11] Richard J-P 1986 Sensitivity of a 1200-kg three mode gravitational radiation detector instrumented with a Clarke or IBM dc squid *J. Appl. Phys.* **60** 3807
[12] Price J C 1987 Optimal design of resonant-mass gravitational wave antennas *Phys. Rev.* D **36** 3555–70
[13] Pang Y and Richard J-P 1992 *Rev. Sci. Instrum.* **63** 56
[14] Solomonson N, Johnson W W and Hamilton W O 1992 Comparative performance of two-, three and four-mode gravitational radiation detectors *Phys. Rev.* D **46** 2299–308
[15] Fisher M A, Bocko M F, Zhang G Z, Marchese L E, Karim M and Bordoni F 1991 Novel transducers for resonant bar detectors *Gravitational Astronomy: Instrument Design and Astrophysical Prospects* ed D E McClelland and H A Bachor (Singapore: World Scientific) pp 317–32
[16] Veitch P J 1991 Parametric transducers *The Detection of Gravitational Waves* ed D G Blair (Cambridge: Cambridge University Press) pp 186–225
[17] Tobar M E and Blair D G 1993 Parametric transducers for resonant bar gravitational wave antennas *J. Appl. Phys.* D
[18] Tobar M E, Linthorne N P and Blair D G 1991 Modelling of a resonant bar antenna with a parametric transducer *Gravitational Astronomy: Instrument Design and Astrophysical Prospects* ed D E McClelland and H A Bachor (Singapore: World Scientific) pp 368–78
[19] Blair D G, Linthorne N P, Mann A G, Peng H, Sebo K, Tobar M E and Turner P J 1991 Progress in optimising a high Q resonant bar antenna *Gravitational Astronomy: Instrument Design and Astrophysical Prospects* ed D E McClelland and H A Bachor (Singapore: World Scientific) pp 172–88
[20] Blair D G, Heng I S, Ivanov E N, van Kann F, Linthorne N P, Tobar M E and Turner P J 1995 Operation of the Perth cryogenic resonant-bar gravitational wave detector *Proc. First Amaldi Conf. on Gravitational Wave Experiments () 1994* to be published
[21] Tobar M E 1993 Gravitational wave detection and low noise sapphire oscillators *PhD Thesis* The University of Western Australia
[22] Amaldi E, Pizzella P, Rapagnani P, Ricci F, Bonifazi P, Cavallari G, Coccia E and Pallottino G V 1986 Data analysis for a gravitational wave antenna with resonant capacitive transducer *Nuovo Cimento* C **9** 51–73
[23] Tobar M E and Blair D G 1995 Massive and three-mode niobium-sapphire resonant-bar gravitational wave antennas *Proc. 7th Marcel Grossmann Meeting On General Relativity () 1994* to be published
[24] Braginsky V B, Panov V I, Petnikov V G and Popel'nyuk 1977 *Instrum. Exp. Tech.* **20** 269